Optical Anisotropy of Supported Lipid Structures Probed by Waveguide Spectroscopy and Its Application to Study of Supported Lipid Bilayer Formation Kinetics

ARTICLE *in* ANALYTICAL CHEMISTRY · AUGUST 2008

Impact Factor: 5.64 · DOI: 10.1021/ac800988v · Source: PubMed

Anal. Chem. **2008,** *80,* 3666–3676

Optical Anisotropy of Supported Lipid Structures Probed by Waveguide Spectroscopy and Its Application to Study of Supported Lipid Bilayer Formation Kinetics

Alireza Mashaghi,[†] Marcus Swann,[‡] Jonathan Popplewell,[‡] Marcus Textor,[†] and Erik Reimhult*[,†]

Laboratory for Surface Science and Technology, Department of Materials, ETH Zurich, Wolfgang-Pauli-Strasse 10, CH-8093 Zurich, Switzerland, and Farfield Group Limited, Farfield House, Southmere Court, Electra Way, Crewe Business Park, Crewe, CW1 6GU, U.K.

Supramolecular conformation and molecular orientation was monitored during supported lipid bilayer (SLB) formation using dual polarization interferometry (DPI). DPI was shown to enable real time sensitive determination of birefringence of the lipid bilayer together with thickness or refractive index (with the other a fixed value). This approach removes differences in mass loading due to anisotropy, so the mass becomes solely a function of the lipid d*n*/d*c* value. DPI measurements show highly reproducible qualitative and quantitative results for adsorption of liposomes of different lipid compositions and in buffers with or without $CaCl_2$. The packing of solvent-free self-assembled SLBs is shown to differ from other preparation methods. Birefringence analysis accompanied by mass and thickness measurements shows characteristic features of vesicle adsorption and SLB formation kinetics previously not demonstrated by evanescent optical techniques, including indications of percolation-type rupture of clusters of liposomes on the surface and correlated adsorption kinetics induced by liposome charge repulsion. Our study demonstrates that understanding of mechanistic details for an adsorption process for which conformational changes and ordering occur can be elucidated using DPI and greatly enhanced by modeling of optical birefringence. The data is in some respects more detailed than what can be obtained with conventional biosensing techniques like surface plasmon resonance and complementary to methods such as the quartz crystal microbalance.

Our present picture of cell membranes as lipid bilayers is the legacy of a century's study. Despite the long history, many fundamental questions about the structure and dynamics of these membranes have not yet been answered, mostly due to the technical hurdles that working with them presents. Recent developments in optical technologies and spectroscopy (e.g., solid state NMR) have raised the hope to unravel such long standing questions.[1]

Over the past few years, the field of membrane biophysics has gained new momentum. Dozens of membrane components have been crystallized and their detailed structures have been uncovered. Recent findings suggest that the 1972 model by Singer and Nicholson needs to be revised in many respects.[2] For instance, bilayers vary considerably in thickness. Orientation of molecules in the bilayer is not as simple as previously expected. Hydrophobic helixes with hydrophilic endings (and possibly other amphipathic species) are not necessarily arranged perpendicular to the membrane plane,[3] and dynamic rearrangement of geometrical distribution is believed to be of even higher importance.[4,5]

In view of the importance of molecular orientation and geometric properties of membranes (e.g., thickness), detailed studies of some simple membrane models may shed light on the complexity of the structure and dynamics of biomembranes. An important model system mimicking cell membranes is the so-called supported lipid bilayer (SLB), which is a planar lipid membrane supported on a solid substrate, typically the surface of a biosensor allowing detailed measurements of its properties and its interaction with peptides and other important biomolecules.

SLBs are commonly prepared by a method pioneered by McConnell et al.[6] in which vesicles in a bulk liquid are allowed to interact with a suitable surface, the latter inducing rupture and fusion of the vesicles to a coherent planar bilayer. This method has advantages over other common preparation techniques like solvent spreading and Langmuir−Blodgett deposition in that it avoids any risk of incorporation of solvents which alter the properties of the membrane and naturally leads to a membrane where the lipid density and structure is determined by the intermolecular forces between the lipids. The pathway to spontaneous formation of SLB by this approach has been shown to often go through three consecutive main phases:[7–11] (i) initially,

* Corresponding author. Tel.: +41 44 633 75 47. Fax: +41 44 633 10 27. E-mail: erik.reimhult@mat.ethz.ch.

[†] ETH Zurich.

[‡] Farfield Group Limited.

(1) Edidin, M. *Nat. Rev. Mol. Cell Biol.* **2003**, *4*, 414–418.
(2) Engelman, D. M. *Nature* **2005**, *438*, 578–580.
(3) von Heijne, G. *Nat. Rev. Mol. Cell Biol.* **2006**, *7*, 909–918.
(4) Mossman, K.; Groves, J. *Chem. Soc. Rev.* **2007**, *36*, 46–54.
(5) Mossman, K. D.; Campi, G.; Groves, J. T.; Dustin, M. L. *Science* **2005**, *310*, 1191–1193.
(6) McConnell, H. M.; Watts, T. H.; Weis, R. M.; Brian, A. A. *Biochim. Biophys. Acta* **1986**, *864*, 95–106.
(7) Keller, C. A.; Glasmastar, K.; Zhdanov, V. P.; Kasemo, B. *Phys. Rev. Lett.* **2000**, *84*, 5443–5446.
(8) Reimhult, E.; Zach, M.; Hook, F.; Kasemo, B. *Langmuir* **2006**, *22*, 3313–3319.

10.1021/ac800027s CCC: $40.75
Published on Web 04/19/2008

only vesicles populate the surface; (ii) at a critical coverage vesicles start to rupture and fuse to form bilayer islands coexisting with vesicles and bare surface; (iii) finally, a coherent SLB is formed, which covers the whole surface. For some systems one or more of these distinct intermediate steps can be suppressed.[9]

The planar bilayer formation process on SiO_2 has previously been extensively investigated by quartz crystal microbalance with dissipation monitoring (QCM-D),[7–9,11–13] but also by e.g. surface plasmon resonance (SPR),[7,8] ellipsometry,[13] fluorescence microscopy,[14] and atomic force microscopy (AFM)[8,13,15] and combinations thereof. It is only in recent years that a detailed understanding of the structural intermediates of SLB formation from liposomes is emerging from both experimental and theoretical studies, though many issues about the formation of SLBs remain to be explored.[9] In spite of the above work where factors such as vesicle size,[12,14–16] experimental temperature and melting transition of lipids,[10,12,17,18] liposome charge,[11,19–21] substrate chemistry,[8,9,11,12,15,16,19,22–25] and influence of pH and counterions have been investigated,[9,11,17,19–21,26] we do not have a complete understanding of the driving forces of the SLB-formation process. In particular, the role of the solid support in the rupture of vesicles and the promotion of SLB formation remains poorly understood beyond the qualitative influence of electrostatic attraction and repulsion. In this respect it has been previously demonstrated that silicon nitride that has been exposed to oxidizing cleaning exhibits the same adsorption and SLB-formation characteristics as SiO_2,[12] which both show the above-described three-step SLB formation kinetics for a large range of lipid composition and buffer conditions. However, the number of liposome systems that have been investigated in detail is still very limited and restricted to phospholipids. Since recent papers have shown that, e.g., the strength and nature of the electrostatic interaction between liposomes and substrate might affect the three-step kinetics described above,[9,11,19–21,26] it is important to further explore this qualitatively and quantitatively. Also, the understanding of the initial phase of liposome rupture is currently very poor, and neither the nature of nor the variations in the so-called critical coverage of liposomes needed for rupture to be initiated or how it propagates is known. An advance in screening techniques allowing for observation of propagation of liposome rupture and SLB formation at increased sensitivity is thus of high interest.

Functionalization of biosensor interfaces with SLBs requires knowledge not only about their formation but also about how the biosensor itself responds to the presence of a bilayer and conformational changes within it. Of the above-mentioned techniques QCM-D has been the most successful in elucidating the vesicle to SLB rupture transformation due to the possibility to distinguish vesicles and SLB on the surface from the different transducer response to each species. Similar success has not been the case for kinetic measurements using waveguide spectroscopy, as evidenced by the lack of such reports in the literature, despite the fact that waveguide spectroscopy techniques—in contrast to SPR—also should be able to distinguish a vesicular film from an SLB based on the simultaneous measurement of thickness and refractive index of the film.

The most common optical biosensing techniques, like waveguide spectroscopies and SPR, make use of a polarized evanescent optical field at the sensor interface. Alignment of lipids orthogonal to the substrate, as in the case of SLB formation, significantly changes the effective refractive index of the lipids as probed by linearly polarized evanescent fields.[27–32] The assumption of an isotropic SLB refractive index leads to incorrect determination of film thickness and the estimated mass of the SLB, as recently addressed theoretically for thin anisotropic films by Horváth and Ramsden.[33] Here these problems are addressed using the technique of dual polarization interferometry (DPI). DPI is a label free, quantitative approach, similar to for example optical waveguide lightmode spectroscopy (OWLS) and coupled plasmon waveguide resonance (CPWR) spectroscopy, that allows real time adsorption measurement. Unlike SPR, where only a single polarized light mode (TM) can excite the surface plasmons and consequently thickness and refractive index cannot be measured independently, two independent measurements with two different polarizations can be performed by DPI, leading to high-resolution determination of thickness *and* refractive index for an isotropic film. For anisotropic films further parameters have to be measured and used in the analysis, which for example can be done *in situ* using coupled plasmon waveguide resonance spectroscopy or by use of complementary data as described in the present work.

Previously, DPI has been demonstrated for the monitoring of, e.g., protein adsorption,[34,35] vesicle deformation[21] and lipid membrane formation.[36–38] Here, we apply this technique to study SLB formation, i.e., measuring optical properties and mass of the lipid structures during SLB formation. CPWR and OWLS have

(9) Richter, R. P.; Berat, R.; Brisson, A. R. *Langmuir* **2006**, *22*, 3497–3505.
(10) Reimhult, E.; Hook, F.; Kasemo, B. *Phys. Rev. E* **2002**, 66.
(11) Rossetti, F. F.; Bally, M.; Michel, R.; Textor, M.; Reviakine, I. *Langmuir* **2005**, *21*, 6443–6450.
(12) Reimhult, E.; Hook, F.; Kasemo, B. *Langmuir* **2003**, *19*, 1681–1691.
(13) Richter, R. P.; Brisson, A. R. *Biophys. J.* **2005**, *88*, 3422–3433.
(14) Johnson, J. M.; Ha, T.; Chu, S.; Boxer, S. G. *Biophys. J.* **2002**, *83*, 3371–3379.
(15) Reviakine, I.; Brisson, A. *Langmuir* **2000**, *16*, 1806–1815.
(16) Reimhult, E.; Hook, F.; Kasemo, B. *J. Chem. Phys.* **2002**, *117*, 7401–7404.
(17) Seantier, B.; Breffa, C.; Felix, O.; Decher, G. *J. Phys. Chem. B* **2005**, *109*, 21755–21765.
(18) Seantier, B.; Breffa, C.; Felix, O.; Decher, G. *Nano Lett.* **2004**, *4*, 5–10.
(19) Richter, R.; Mukhopadhyay, A.; Brisson, A. *Biophys. J.* **2003**, *85*, 3035–3047.
(20) Rossetti, F. F.; Textor, M.; Reviakine, I. *Langmuir* **2006**, *22*, 3467–3473.
(21) Khan, T. R.; Grandin, H. M.; Morozov, A. N.; Mashaghi, A.; Textor, M.; Reimhult, E.; Reviakine, I. In press, *Biointerfaces*.
(22) Csucs, G.; Ramsden, J. J. *Biochim. Biophys. Acta-Biomembr.* **1998**, *1369*, 61–70.
(23) Keller, C. A.; Kasemo, B. *Biophys. J.* **1998**, *75*, 1397–1402.
(24) Reimhult, E.; Larsson, C.; Kasemo, B.; Hook, F. *Anal. Chem.* **2004**, *76*, 7211–7220.
(25) Richter, R. P.; Brisson, A. *Langmuir* **2004**, *20*, 4609–4613.
(26) Richter, R. P.; Maury, N.; Brisson, A. R. *Langmuir* **2005**, *21*, 299–304.
(27) Csucs, G.; Ramsden, J. J. *Biochim. Biophys. Acta—Biomembr.* **1998**, *1369*, 304–308.
(28) Horvath, R.; Fricsovszky, G.; Papp, E. *Biosens. Bioelectron.* **2003**, *18*, 415–428.
(29) Ramsden, J. J. *J. Phys. Chem.* **1993**, *97*, 4479–4483.
(30) Salamon, Z.; Devanathan, S.; Alves, I. D.; Tollin, G. *J. Biol. Chem.* **2005**, *280*, 11175–11184.
(31) Salamon, Z.; Lindblom, G.; Tollin, G *Biophys. J.* **2003**, *84*, 1796–1807.
(32) Salamon, Z.; Tollin, G. *Biophys. J.* **2001**, *80*, 1557–1567.
(33) Horvath, R.; Ramsden, J. J. *Langmuir* **2007**, *23*, 9330–9334.
(34) Swann, M. J.; Peel, L. L.; Carrington, S.; Freeman, N. J. *Anal. Biochem.* **2004**, *329*, 190–198.
(35) Cross, G. H.; Reeves, A. A.; Brand, S.; Popplewell, J. F.; Peel, L. L.; Swann, M. J.; Freeman, N. J. *Biosens. Bioelectron.* **2003**, *19*, 383–390.
(36) Popplewell, J. F.; Swann, M. J.; Freeman, N. J.; McDonnell, C.; Ford, R. C. *Biochim. Biophys. Acta—Biomembr.* **2007**, *1768*, 13–20.

previously been used to analyze properties of SLB assembled by Langmuir−Blodgett deposition,[28,39] liposome interaction[22] and by solvent spreading[30–32] using waveguide spectroscopy. However, in these studies solvent-free membranes and detailed formation kinetics were never addressed. We introduce a method for determining the birefringence of the bilayer together with thickness or refractive index (with the other a fixed value) using DPI, but which could also be applied to other waveguide spectroscopy configurations with equal sensitivity. By using the anisotropy to calculate the isotropically averaged refractive index for each time point, it is possible to remove differences in mass loading originating from overestimation or underestimation of the film refractive index by directional probing, so the mass becomes solely a function of, e.g., a single lipid dn/dc value. By analyzing the birefringence as function of adsorption time and lipid surface coverage, very sensitive and distinct measurements of vesicle and SLB coverage during the course of the rupture process can be made. This analysis correlates very well with complementary QCM-D measurements as well as providing new detailed observations of the difference in the vesicle to SLB transition for different lipid compositions and environmental conditions. The latter was exemplified by investigations of the effects of divalent cations, lipid shape, charge of the headgroup and the temperature on alignment, packing and thickness of the membrane as well as on the mechanism of lipid bilayer formation. The high sensitivity of the method compared to previous approaches to study SLB formation kinetics also led to observations of fluctuations in the vesicle population on the surface, which also were shown to vary between different lipid compositions.

EXPERIMENTAL SECTION

DPI Analysis. DPI, as deployed in *Ana*light BIO200 (Farfield Group Ltd., United Kingdom), consists of a dual slab waveguide sensor chip (22 mm × 6 mm) illuminated with an alternating polarized laser beam (wavelength 632.8 nm). The chip consists of a four layer dielectric stack of silicon oxinitride on a silicon wafer surface and works as an integrated Young's interferometer, generating interference fringes at its output. DPI measures the spatial changes of an interference pattern as material is deposited in the region of the evanescent field close to the surface of the top waveguide layer. The change in refractive index within the evanescent field accompanying material deposition changes the optical path length of the top waveguide and causes a relative phase shift observable as a shift of the interference fringes. By exciting the chip with two orthogonal polarizations, exciting TE and TM waveguide modes, two separate measurements of fringe shifts are made (see Figure 1).[34,35,40]

Using a minimization algorithm and calculating the propagation constants for the light in the calibrated optical structure, the dimensions of an adsorbed isotropic single layer (n and d) are determined by fitting to the measured phase changes.[35,41]

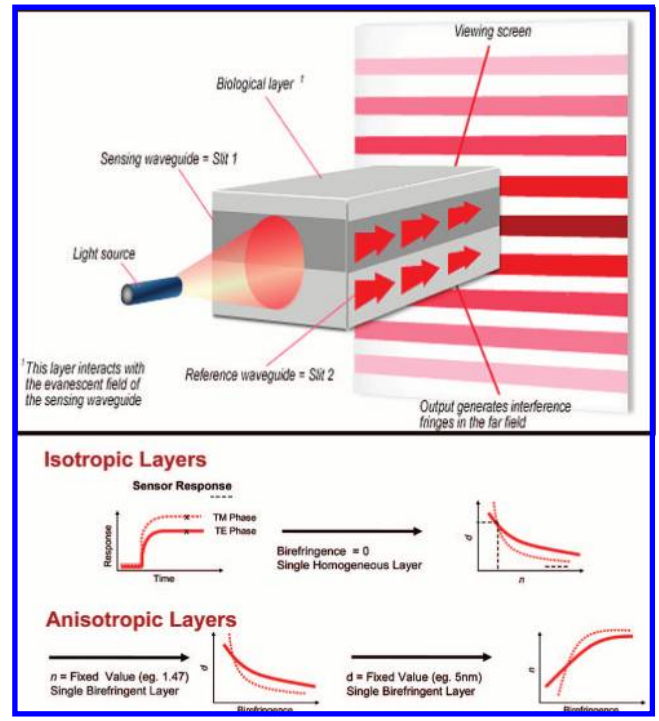

Figure 1. Schematics of a dual polarization interferometry sensor and the basis for its analysis. Using information from both the absolute and relative changes in optical path length for propagation of two waveguide modes, the thickness and refractive index of an adsorbed layer can be determined; or if one of them is known the degree of anisotropy determined.

With an anisotropic overlayer, the refractive index perpendicular to the surface (commonly defined as the extraordinary refractive index, n_e) is different from that parallel to the surface (ordinary refractive index, n_o), the difference between the two being termed the birefringence. This will introduce an additional unknown through the difference in effective refractive indexes of the layer in the plane or orthogonal to the plane of the waveguide, n_{TM} and n_{TE} measured by the two waveguide modes. The analysis can be replicated by instead fixing one of n, d or $n_{TM} - n_{TE}$ to determine the other two from the measured change in propagation constants for the two modes. Strictly, the TM mode is affected by the adlayer thickness and both n_e and n_o ($n_{TM} = (n_e^2 \sin^2\theta + n_o^2 \cos^2\theta)^{1/2}$, where θ is the mode angle, $N_{eff} = N_g \sin\theta$, N_{eff} the waveguide effective index and N_g the guiding layer index), while the TE mode is affected only by the layer thickness and n_o ($n_o = n_{TE}$).[33] Since the propagation constants for the two modes in the device are known, n_o and n_e can be calculated from n_{TM} and n_{TE}. However, in practice, we can assume $n_e \approx n_{TM}$ because the contribution of n_o to the TM mode is small (e.g., for our current measurements this will introduce an error of ~0.1% in the calculated mass and discrepancy of ~2% between the calculated "effective birefringence", $n_{TM} - n_{TE}$, and the layer birefringence, $n_e - n_o$).

The fitting of the data is obtained by calculating the respective effective adlayer refractive indexes, n_{TM} and n_{TE}, for each mode corresponding to the measured phase shift by solving the waveguide equations given an assumed thickness of the lipid

(37) Terry, C. J.; Popplewell, J. F.; Swann, M. J.; Freeman, N. J.; Fernig, D. G. *Biosens. Bioelectron.* **2006**, *22*, 627–632.
(38) Popplewell, J.; Freeman, N.; Carrington, S.; Ronan, G.; McDonnell, C.; Ford, R. C. *Biochem. Soc. Trans.* **2005**, *33*, 931–933.
(39) Voros, J.; Ramsden, J. J.; Csucs, G.; Szendro, I.; De Paul, S. M.; Textor, M.; Spencer, N. D. *Biomaterials* **2002**, *23*, 3699–3710.
(40) Cross, G. H.; Reeves, A.; Brand, S.; Swann, M. J.; Peel, L. L.; Freeman, N. J.; Lu, J. R. *J. Phys. D—Appl. Phys.* **2004**, *37*, 74–80.
(41) Cross, G. H.; Ren, Y. T.; Freeman, N. J. *J. Appl. Phys.* **1999**, *86*, 6483–6488.

bilayer. A constant thickness corresponding to the steric thickness obtained by neutron scattering is for simplicity assumed for the entire process.[42] A thickness of 4.7 nm is thus assumed for the POPC SLB, 4.5 nm for the DOPC and 4.4 for the DMPC SLB formation processes at 30 °C.[42] For an anisotropic film of the same thickness or for an isotropic layer of different thickness this fitting will result in a different n obtained for the TM and TE modes respectively. If the correct thickness is used as input (as should be the case for the fully formed SLB) the obtained difference $n_{TM} - n_{TE}$ will correspond to the true effective birefringence of the overlayer. During the parts of the process dominated by adsorbed vesicles the Ansatz thickness will underestimate the true thickness and the calculated birefringence mainly results from polarization across the entire vesicle and not from interior alignment of the molecular constituents. A corresponding analysis can be performed if for example either the anisotropy or the isotropic refractive index is well-known by keeping that quantity fixed instead. Between 3 and 6 measurements were used to calculate the mean values and SEM for each system for which data is presented.

In order to calculate the adsorbed mass, the average or corresponding isotropic value of the refractive index has to be calculated according to $n_{iso} = ((n^2_{TM} + 2n^2_{TE})/3)^{1/2}$. By relying on a single mode the mass would be either over- or underestimated. The mass of the adsorbed layer can then be obtained by the de Feijter formula $m = d(n_{iso} - n_{buffer})/(dn/dc)_{lipid}$.[43] The $(dn/dc)_{lipid}$ is however not well-known, and an equivalent alternative model was used for convenience, assuming a commonly used approximate fixed isotropic refractive index of the lipid film of 1.47. Given the refractive index the corresponding thickness that yields the observed phase shift for each mode can be fitted as described above. The "isotropic thickness" can now be calculated as $d_{iso} = ((d_{TM} + 2d_{TE})/3)^{1/2}$ and assuming a reasonable density of lipids of 1.05 g/cm^3 an approximate mass for the SLB can be calculated as $m = 1.05 \times d_{iso} \times 100$ (ng/cm^2). This is equivalent to choosing a $(dn/dc)_{lipid} \approx 0.135$ (cm^3/g). We emphasize that with the current uncertainties regarding the $(dn/dc)_{lipid}$ or ρ_{lipid} we do not consider this a precise measurement of the lipid mass on the waveguide surface, nor find it useful to push further to obtain this value for the present study since it does not affect the presented analysis. The mass values are only calculated to obtain an approximate value and for comparison of adsorbed mass between the different systems under investigation.

QCM-D Experiments. Quartz crystal microbalance with dissipation monitoring (QCM-D)[44] was used as a well-known complementary method to study liposome adsorption and SLB formation kinetics using a Q-Sense E4 (Q-Sense AB, Sweden).[9] The QCM-D measures the change in resonance frequency, Δf, and the change in damping or energy dissipation, ΔD, of a piezoelectric quartz crystal oscillator sensor in real time. While Δf is roughly proportional to adsorbed mass including coupled water, ΔD provides a sensitive measure of the supramolecular conformation of the adsorbed film. For example, an adsorbed SLB does not give a significant contribution to ΔD while adsorbed liposomes increase ΔD substantially.[8,23]

Materials. 1-Palmitoyl-2-oleoyl-*sn*-glycero-3-phospocholine (POPC), 1-palmitoyl-2-oleoyl-*sn*-glycero-3-phospho-L-serine (POPS; sodium salt), 1,2-dioleoyl-*sn*-glycero-3-phospocholine (DOPC), 1,2-dioleoyl-*sn*-glycero-3- phospho-L-serine (DOPS; sodium salt), and 1,2-dimyristoyl-*sn*-glycero-3-phosphocholine (DMPC) were purchased from Avanti Polar Lipids (USA) with a purity >99% and stored at −20 °C. The lipids were dissolved in chloroform. All water used in cleaning and preparations was Milli-Q grade (Millipore, USA). Sodium chloride (purity >99.5%), calcium chloride (purity >99%), ethanol and *N*-2-hydroxyethylpiperazine-*N*′-2-ethanesulfonic acid (HEPES) (purity >99%) were purchased from Fluka Biochemicals (Switzerland). Buffers were prepared from ultrapure water with 10 mM HEPES, 150 mM NaCl with and without 2 mM $CaCl_2$. The pH was set to 7.4 by addition of an appropriate amount of NaOH.

Preparation of Liposomes. Commercial lipid preparations (dissolved in chloroform) were dried to a thin film in a round-bottom flask under a steady stream of N_2. The lipids were resuspended in buffer without $CaCl_2$ at a concentration of ~5 mg/mL, extruded 31 times through double polycarbonate membranes with a pore size of 100 nm (Avestin, Canada). Several different liposomes were prepared: DMPC, POPC, DOPC, POPC:POPS (8:2 mol:mol) and DOPC:DOPS (8:2 mol:mol). The quality of the liposome preparation was determined by measuring the size distribution with dynamic light scattering (Malvern Zetasizer 3000 HAS (Malvern, USA) and checked for SLB formation kinetics using QCM-D.

SLB Formation Experiments. The surfaces (waveguide and SiO_2-coated QCM crystals; both effectively SiO_2 in the top surface layer) were cleaned by SDS (2%; Sigma, Switzerland, purity >99%), water/ethanol and UV−ozone (1 h). After reaching a constant baseline, calibrations were performed for ethanol (80%) and pure water. Liposome samples (50 μg/mL) were infused at a flow rate of 10 μL/min using a syringe pump followed by rinsing with buffer at the same flow rate. All experiments were performed at 25 °C, except for the adsorption of DMPC liposomes at 20 °C, which was conducted at 1 mg/mL concentration and DMPC liposomes also adsorbed at 30 °C as noted in the text.

RESULTS AND DISCUSSIONS

SLB Formation Kinetics by Birefringence Analysis. Plotting the time evolution of the calculated birefringence at a fixed film thickness in order to analyze the kinetics of SLB formation was shown to be a sensitive method. As demonstrated in Figure 2a (showing typical adsorption kinetics for all the lipid systems under investigation) the mass adsorption shows close to linear uptake for the major part of the process, indicating that no significant lipid mass loss occurs from the surface at any point. However, birefringence increases dramatically from zero to a maximum before it drops back to a stable value upon completion of the adsorption. A mixture of POPC:POPS (8:2) in the liposomes is known to result in SLB formation in the presence of 2 mM Ca^{2+},[11] which is demonstrated by the QCM-D measurement in Figure 2b. Interesting to note is that the birefringence peak correlates very well in time with the ΔD peak for experiments performed under identical conditions in this plot. The simultaneous maximum occurs regardless of lipid composition and buffer

(42) Nagle, J. F.; Tristram-Nagle, S. *Biochim. Biophys. Acta—Rev. Biomembr.* **2000**, *1469*, 159–195.
(43) de Feijter, J. A.; Benjamins, J.; Veer, F. A. *Biopolymers* **1978**, *17*, 1759–1772.
(44) Rodahl, M.; Hook, F.; Krozer, A.; Brzezinski, P.; Kasemo, B. *Rev. Sci. Instrum.* **1995**, *66*, 3924–3930.

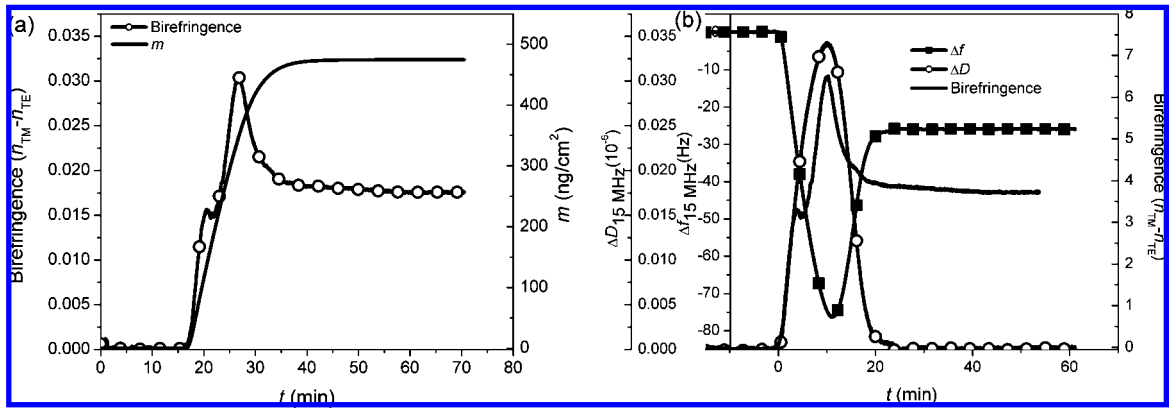

Figure 2. (a) Adsorbed mass, *m*, and birefringence plotted as a function of time for POPC:POPS (8:2) liposome adsorption in the presence of Ca^{2+}. The overshoot of the birefringence occurs slightly before the final mass is reached as demonstrated for this adsorption curve, which is typical for the range of SLB forming lipid systems investigated. (b) Comparison of QCM-D and DPI-birefringence analysis for POPC:POPS (8:2) in the presence of Ca^{2+}. The peak in birefringence coincides closely with the peak in dissipation from QCM-D obtained under the same flow conditions. The dissipation is known to peak at the maximum concentration of liposomes on the surface.[8]

used for all the investigated systems with POPC, DOPC and POPS or DOPS lipids. This strongly indicates that the maximum in birefringence is due to a maximum in the number of intact liposomes on the waveguide surface, as previously demonstrated to be the case for the QCM-D ΔD peak.[8] The mass kinetics can be compared to that observed in the same paper by Reimhult et al., where SPR was used as an evanescent optical sensing technique. The mass uptake measured by SPR, which employs only p-polarized light, is artificially increased during the final one-third of the process due to that the mass transport to the surface gets inflated by the increased proximity to the surface and alignment of the lipid molecules during vesicle rupture.[8] These effects cannot be accounted for with the information obtained using only a single polarization.

In the birefringence evolutions shown in Figures 2 and 3 the layer thickness is kept constant at the thickness of the respective SLB for the calculations based on the collected data. (Thickness values for each respective SLB dependent on lipid composition were selected from published neutron scattering data.[42,45]) Thus, only for the final SLB is the accurate birefringence calculated. Many factors contribute to the difference in polarizability probed by the TM and TE waveguide modes for an adsorbed thin film, e.g., film thickness, distance from the surface, deformation, dielectric constant of the molecules and the surrounding liquid, the electrical double layer and the electrical field components induced by the molecules and surface. While the anisotropic polarizability of the lipids will strongly influence the sensed birefringence of the SLB, the alignment of lipids within the membrane of a liposome yields only a small contribution, since to a first approximation it could be weighted by the lipid volume fraction which for a liposome with low deformation is much smaller than for a planar SLB. The main contribution to the "birefringence" of the liposome layer instead reflects its physical thickness, which appears as birefringence due to the fixed thickness used in the calculation. While for the cases demonstrated in Figure 3 the significantly higher thickness of the liposomes leads to a higher "birefringence" than for the SLB and a pronounced peak for the transition, the method only requires that there is a difference in terms of polarizability of the film for the two waveguide modes between two (or more) states in an investigated process for the tool to be useful for investigating transition kinetics.

Figure 3b–d shows examples of the birefringence and the rate of change in the phase shift ($d\phi/dt$, which has the same functional dependence as dm/dt) versus mass for four investigated systems forming SLB. No plots for DOPC or DOPC:DOPS systems are shown, because they correspond closely to the POPC and POPC:POPS cases, respectively. Figure 3a on the other hand shows the same kind of plot generated for DMPC liposome adsorption. These plots show one advantage of using DPI or other variants of waveguide spectroscopy with this type of analysis over QCM-D, which is the only sensing technique previously employed able to distinguish liposomes from SLB in high real time resolution measurements.[8,9,23,24] As an optical evanescent technique DPI will after correcting for anisotropy yield the true mass of lipids adsorbed on the surface. This is not obtained by an acoustic technique where the measured mass will be distorted by coupled water in the film, which is also the reason why QCM-D shows a contrast between liposomes and SLB. However, by analyzing the evolution of the birefringence (similar to the evolution of the QCM-D dissipation) relative to the simultaneously measured mass uptake kinetics, new insights can be gained into the adsorption and transformation kinetics. In Figure 3 we can thus reveal subtle differences in the mass adsorption kinetics of various lipid–buffer systems on the same surface. Starting with the liposome adsorption in Figure 3a the smooth infilling kinetics and the steady rise in birefringence (obtained by assuming a constant SLB thickness) for the system testify to that no conformational transition occurs during the adsorption process, except some packing in the end phase. All the remaining systems form SLBs and the distinction from the liposome adsorption process is clear in terms of final mass, rate of phase change (infilling behavior) and—most clearly—in the transition kinetics for the birefringence. After initial mixing, $d\phi/dt$ remains at a constant value for mass transport limited adsorption with no changes in the film structure. In a space filling model $d\phi/dt$ will instead have a linear slope intersecting the *x*-axis at full coverage, expected to correspond to the random sequential adsorption (RSA) jamming limit of ~55% for liposomes. These two

(45) Johnson, S. J.; Bayerl, T. M.; McDermott, D. C.; Adam, G. W.; Rennie, A. R.; Thomas, R. K.; Sackmann, E. *Biophys. J.* **1991**, *59*, 289–294.

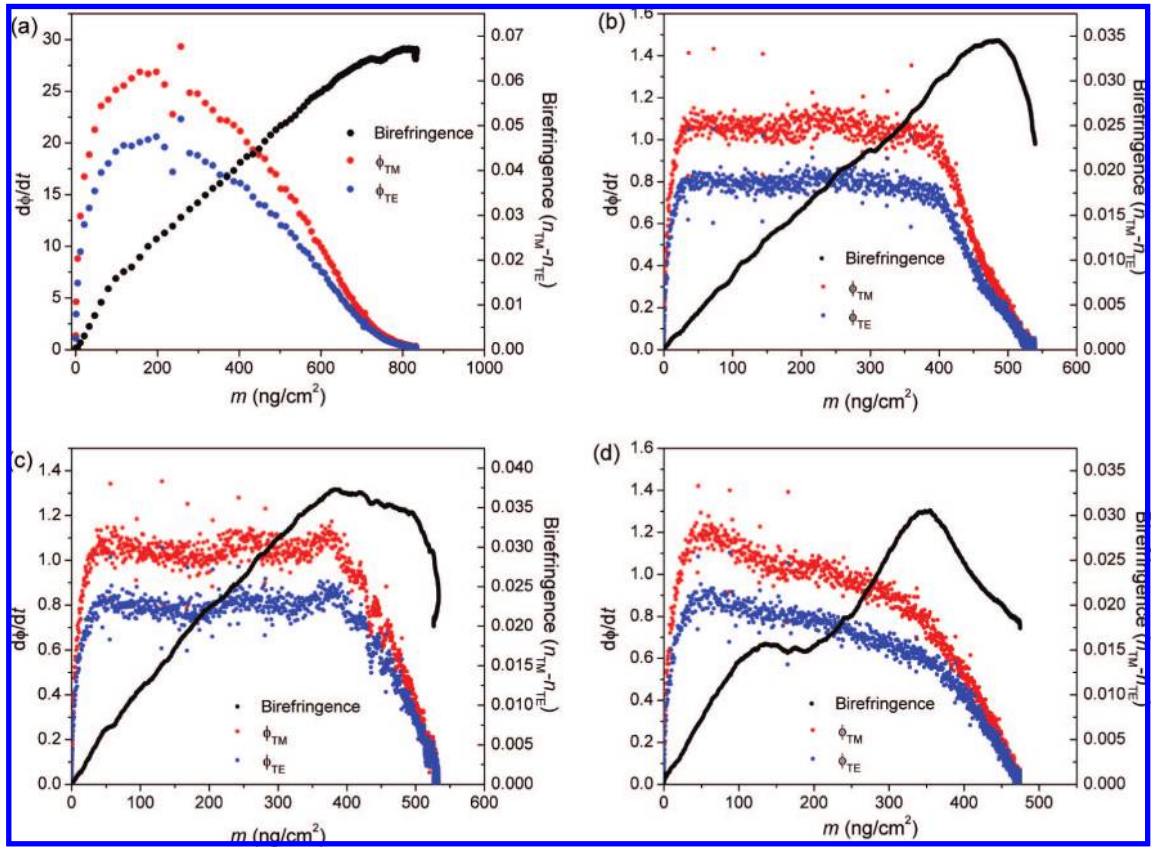

Figure 3. Birefringence and rate of TM and TE phase change, $d\phi_{TM,TE}/dt$, versus mass, m, for (a) DMPC liposome adsorption at 20 °C, (b) POPC, (c) POPC with Ca^{2+} and (d) POPC:POPS (8:2) with Ca^{2+}. The latter three form complete SLBs. The rate of phase change has the same functional dependence as the rate of mass change. It is clear that all SLB forming systems are easily distinguishable from intact lipsome adsorption in terms of final mass, rate of phase change (infilling behavior) and—most clearly—in the transition kinetics for the birefringence. The extrapolation of the second phase in (d) for POPC:POPS (8:2) with Ca^{2+} will lead to a mass of about ($m_{TM} = 1208 \pm 66$, $m_{TE} = 1160 \pm 65$ ng/cm^2) for the random sequential adsorption jamming limit.

qualitatively different behaviors are observed in Figure 3, with POPC vesicles with or without Ca^{2+} present corresponding to mass transport limited adsorption and POPC:POPS liposomes corresponding to space filling. The different adsorption behavior of POPC:POPS liposomes has important implications for interpreting adsorption data on these systems using time to estimate coverage, as has been done in some earlier work. Importantly, it also indicates that the addition of charge to the liposomes not only alters the interaction with the substrate but is also likely to lead to a change in liposome−liposome interaction during adsorption. A plausible interpretation is that liposome−liposome charge repulsion leads to a more correlated adsorption and short-range order similar to what has been observed for charged nanoparticles.[46]

The second interesting observation is that $d\phi/dt$ for all systems changes slope when ~73−77% of the mass coverage has been reached. This change in slope cannot be explained by the adsorption models unless a transformation from liposomes to SLB occurs on the surface. SLB will cover 2−4 times the surface of a liposome. The higher area per adsorbed mass unit will result in a steeper slope and a lower intersect, but since the measured phase shifts also depend on extension and birefringence of the layers as described in this paper, a direct correspondence between the difference in slope and area coverage is not obtained. That the change in slope is related to liposome rupture on the surface dominating the adsorption is demonstrated by that the peak in birefringence for POPC and POPC:POPS occurs synchronized slightly after the change in slope as expected. The case of POPC in the presence of Ca^{2+} is slightly different. Here the maximum in birefringence occurs well after a first change to a steeper slope and instead coincides with a second change to a lower slope. However, it is clear that the two ways of analyzing the data support each other and that DPI allows analysis of adsorption processes involving conformational changes affecting mass distribution and surface coverage alternatively by studying the mass coverage kinetics and/or the birefringence evolution of the system. The observed 73−77% of the SLB mass observed at the point of change in slope also agrees very well with an earlier determination of the amount of lipid mass at the critical coverage for rupture of POPC liposomes of 77 ± 5%, corresponding to ~30% of the surface area covered by adsorbed liposomes.[8] The presented results thus indicate a very similar critical coverage also for several other SLB forming systems that vary significantly in terms of the dominating electrostatic interaction between liposome and substrate.

Observation of Fluctuations during Liposome Adsorption and Rupture. The transient maximum in birefringence observed for all SLB forming systems displayed variation in amplitude depending on lipid composition and buffer, as is exemplified in

(46) Hanarp, P.; Sutherland, D. S.; Gold, J.; Kasemo, B. *Colloid Surf. A—Physicochem. Eng. Asp.* **2003**, *214*, 23–36.

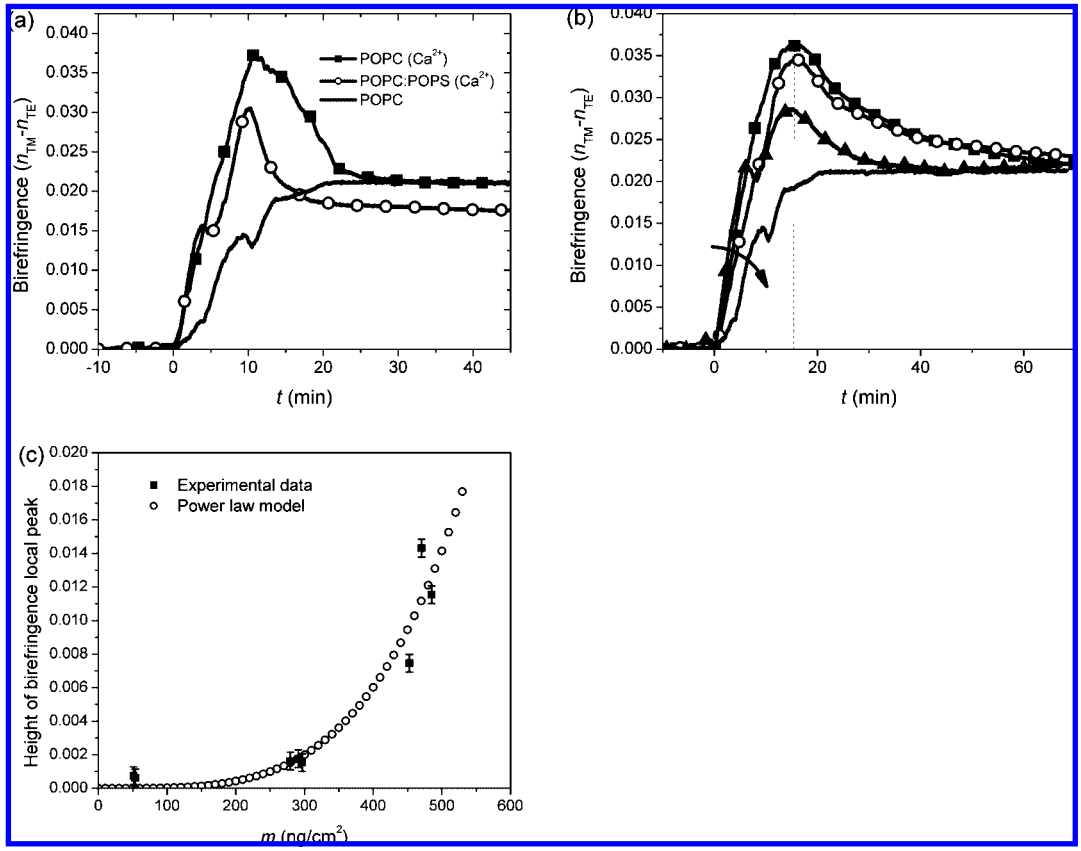

Figure 4. (a) Evolution of birefringence during SLB formation for the three different classes of liposome and buffer combinations under study. (b) POPC SLB formation followed several related kinetic pathways with comparable probability, of which a selection of 4 different pathways for the same adsorption conditions are shown. Variation was observed in birefringence rate of increase and peak birefringence height, but not substantially in peak position. (c) Height of birefringence spikes observed in the oscillations occurring during the vesicle adsorption phase versus adsorbed mass for POPC vesicles. The spike heights follow a power law as expected for a percolation system.

the upper panel of Figure 4a for the three systems with POPC as major constituent. The addition of 2 mM Ca^{2+} to the buffer leads to an average increase in the overshoot of the peak, regardless of investigated lipid compositions.

While POPC yielded similar or higher overshoots than POPC:POPS when Ca^{2+} was present, there was significant variability in the overshoot height of POPC without Ca^{2+}. This variability correlated with another highly reproducible feature of the birefringence plots. The continuous initial increase in birefringence could be interrupted by sudden drops as seen in Figure 4a,b and which occur especially clearly for POPC without Ca^{2+}. Figure 4b exemplifies that the occurrence of drops or fluctuations in the rate of increase in the birefringence correlates with a suppression of peak height and a decrease in average slope. Both the number and the height of the fluctuations decrease the peak height, which for some measurements on POPC without Ca^{2+} was completely suppressed. The different kinetic paths to a fully formed SLB indicated by this occur with comparable probability. While variations in the mass and the birefringence of the SLB end state are small, there is a correlation between peak height and longer rupture phase for the liposomes (time between maximum in birefringence and steady state for the SLB, *cf.* Figure 4) and slightly higher mass for the SLB. But as exemplified by the selection of measurements in Figure 4b, the position in time for the peak is relatively constant. In a few cases a small mass loss could be detected in the end phase as for the high peak curves in Figure 4b. Since there is also a very slight increase in birefringence with the higher mass, this could be interpreted as that the less efficient rupturing process evidenced by the slow rupture phase leads to a small number of vesicles still present on the surface after equilibration.

A detailed analysis and interpretation of the fluctuations is under development and will be published elsewhere, but a possible scenario for its origin will be briefly described. It has previously been established that the PC and PC:PS lipid systems investigated here will adsorb randomly to an SiO_2 surface[9,19] and rupture at a critical coverage.[7,8,47] This is, however, a macroscopic manifestation of what must be a collection of microscopic rupture events where clusters of tightly packed liposomes rupture and spread. The clusters govern the macroscopic behavior of the system as in percolation models.[48] Clusters with a size close to the typical cluster size dominate the behavior of the system as the system approaches percolation transition,[48] in this case equivalent to the macroscopically detectable liposome rupture event. The oscillations, or spikes, in the birefringence are manifestations of concerted rupture of clusters present in the system. As the surface coverage increases and gets closer and closer to percolation coverage, the average size of the clusters and typical cluster size increase.

(47) Zhdanov, V. P.; Keller, C. A.; Glasmastar, K.; Kasemo, B. *J. Chem. Phys.* **2000**, *112*, 900–909.
(48) Stauffer, D. *Phys. Rep.—Rev. Sec. Phys. Lett.* **1979**, *54*, 1–74.

In this case, fluctuations may lead to macroscopically observable effects. Using a percolation model, a power scaling of the amplitude of birefringence spikes in the oscillations with surface coverage would be expected and also seems to be observed as a first approximation in Figure 4c. This behavior has previously not been observed by for example QCM-D and other real-time sensing techniques,[9] which could be due to either a higher sensitivity to fluctuations in the birefringence than in the QCM-D dissipation or that the long linear sampling length of the DPI flow channel creates larger variation in cluster size along the channel than in the circular and shorter flow geometry of a QCM-D measurement cell.

Since the SLB formation kinetics seem to fit a percolation model, an explanation can be proposed for why the charged POPC:POPS liposomes show smaller fluctuations than the POPC liposomes. The adsorption of charged liposomes will be more correlated due to charge interactions, which was also indicated from the mass adsorption kinetics discussed above. Less randomness in the positioning of liposomes on the surface will lead to a more stable and homogeneous distribution of the cluster size up to the percolation transition. This would result in lower variability and higher incidence of overshoot in the birefringence, the latter corresponding to a more "monodisperse" critical cluster size.

Optical Properties and Thickness of SLB. It is expected that SLBs reveal different thickness and optical properties depending on their composition and also on the presence of divalent cations like Ca^{2+} which can influence the ordering and packing of the lipids. We investigated these features in detail for the following vesicles: POPC, POPC:POPS (8:2), DOPC, DOPC:DOPS (8:2) and DMPC in the presence and absence of 2 mM $CaCl_2$. These lipids differ significantly with respect to the charge of the head groups, their shapes and the nature and stoichiometry of their interaction with calcium ions. The highly reproducible results are shown in Table 1.

First of all, a comparison can be made of the here obtained values for refractive index and birefringence with those of earlier studies employing different waveguide setups and analysis. Such a comparison is of interest since previous work has been carried out on lipid bilayers obtained either by Langmuir−Blodgett deposition[27–29] or by solvent spreading,[30–32] and thus not by the convenient, solvent-free, method of self-assembly from liposomes directly on the substrate used in this work. Langmuir−Blodgett deposition can easily lead to incomplete coverage or a high amount of defects that will both lower the mass density (and thus the film refractive index) and the alignment of the lipids in the film. A comparison of the values in Table 1 to those obtained by optical lightmode waveguide spectroscopy by Ramsden[29] and Horváth et al.[28] seems to support this suggestion. For example, Ramsden, who also studied a POPC lipid bilayer, obtained a substantially lower $n \approx 1.376$ and a birefringence of 0.005 for POPC.[29] Ramsden showed already in 1993 that incorporation of organic solvent into the membrane has an ordering effect on the membrane.[29] The refractive index will increase as will the birefringence. Thus a comparison with membranes obtained by the common method of solvent spreading might yield a lower value for refractive index and birefringence. Salamon et al. have in a number of careful studies used plasmon-coupled waveguide resonance to study lipid bilayers spread with solvents in a thin Teflon orifice. For these

Table 1. Isotropic Refractive Index, Thickness and Birefringence for Different SLBs and One Example of Liposome Layer with SEM Given in Parentheses[a]

	POPC SLB	POPC SLB (Ca^{2+})	POPC:POPS SLB (Ca^{2+})	DOPC SLB	DOPC SLB (Ca^{2+})	DOPC:DOPS SLB (Ca^{2+})	DMPC liposomes (20 °C)	DMPC SLB (20 °C)	DMPC SLB (30 °C)
n	1.4788 (2.8e−3)	1.4782 (1.2e−3)	1.4711 (1.4e−3)	1.456 (2.5e−3)	1.4693 (4.2e-3)	1.4904 (3.6e−3)	1.36049	1.4810	1.47378
birefringence ($n_{TM} - n_{TE}$)	0.02164 (5.3e−4)	0.01960 (3.5e−4)	0.01955 (7.1e−4)	0.01586 (7.4e−4)	0.0139 (2.1e−3)	0.0250 (1.9e−3)	N/A	0.0231	0.02004
thickness (nm)	4.976 (9.9e−2)	4.962 (4.3e−2)	4.689 (5.5e−2)	3.992 (8.4e−2)	4.46 (1.4e−1)	5.2855 (5.1e−3)	56.38	4.980	4.524

[a] The thickness is calculated by modeling the response for both TE and TM modes using the same assumed isotropic refractive index ($n = 1.47$) and is thus not expected to correspond exactly to the true thickness. This will also result in a different apparent thickness for the two modes. The thicknesses obtained for TM and TE modes are weighted isotropically analogously to the approach used for the refractive index. The isotropic refractive index and birefringence are modeled assuming a fixed thickness of 4.7 nm for POPC (POPS), which has been determined by neutron scattering as the steric thickness for DPPC lipid bilayers and should be a good estimate also for POPC SLBs.[42,45] DOPC (DOPS) was modeled using a fixed thickness of 4.5 nm similarly determined by neutron scattering.[42] For DMPC liposomes a comparison value is given for the refractive index and thickness (no or low birefringence exists) of a vesicular layer formed at 20 °C (below the gel-to-liquid phase transition temperature). This can be compared to the values calculated for DMPC SLBs at 20 °C (gel phase) and 30 °C (liquid crystalline phase) calculated assuming literature steric thickness values for the SLBs at these temperatures obtained by neutron scattebring,[42] 4.4 and 4.6 nm for 30 and 20 °C respectively.

measurements unusually high lipid surface densities (lipid headgroup areas as small as ~50 Å^2) with corresponding high thickness and refractive index values of $d = 5.2$ nm and $n = 1.489$, and a birefringence of 0.0556, have been obtained for POPC lipid bilayers.[32] Thus, while the obtained refractive index does not differ much from what was obtained in our study, mass per area and orthogonal alignment are substantially higher leading to higher packing than what is usual for a noncompressed SLB. The comparison with our results for self-assembled solvent-free membranes demonstrates the importance of characterizing the properties for membranes using the particular assembly method of interest. With increased focus on self-assembly of low-defect solvent-free membranes suitable for incorporation of a wide range of transmembrane proteins, the results presented in Table 1 are an important contribution to cataloguing the properties of such membranes for functionalization of optical biosensors.

Birefringence involves contributions from both the shape of the molecule and its molecular polarizability tensor.[32] Polar head groups are commonly assumed to have a much more isotropic polarizability tensor than the nonpolar chains,[49] and therefore they have a much smaller effect on the refractive index anisotropy.[32] Chain alignment should thus play a significant role for the measured birefringence. It has been proposed that, although Ca^{2+} would interact in the headgroup region, the saturation of the alkyl chains will affect the degree of ordering that occurs for PC lipids. Presence of Ca^{2+} reduces the SLB birefringence for both POPC and DOPC, although the statistically certain change is small. A small decrease should imply less orthogonal alignment of the chain region relative to the surface plane. Interestingly, the isotropically weighted refractive index—proportional to the mass at constant thickness—stays the same with Ca^{2+} for POPC but increases significantly for DOPC. This results in that while there is a general correlation between higher refractive index and a higher birefringence, DOPC with and without Ca^{2+} does not follow this trend. A correlation of birefringence with isotropic refractive index can be expected based on simple arguments of increased chain packing leading to higher orthogonal alignment of the lipids when the mass density (refractive index) is higher. However, for DOPC with Ca^{2+} the orthogonal alignment of the lipids is slightly decreased despite the high increase in mass density. The adsorption of Ca^{2+} ions to SiO_2 is negligible and the same for all systems, so the main effect of Ca^{2+} will be from its influence on direct interaction between the lipids,[50] despite that on average only ~0.1% of all DOPC lipids should be occupied by a Ca^{2+} ion under the experimental conditions.[51,52] It is interesting to note that, from a consideration of the molecular dimensions of DOPC and POPC, a lower SLB thickness of ~5% for DOPC is expected. If the birefringence is assumed equal between the two SLBs (e.g., an isotropic layer assumed), the thickness is ~25% thinner in the absence of Ca^{2+} and ~13.5% thinner in the presence of Ca^{2+} for DOPC versus POPC. No such large differences have been observed in corresponding QCM-D measurements of the hydrated thickness. The additional large difference measured for the anisotropy of the bilayer is thus likely explained by a strong but off-normal alignment of the DOPC allowing high packing in the presence of Ca^{2+} and what seems to be a substantially lower packing than for POPC without Ca^{2+}.

Not surprisingly, calcium affects POPC:POPS and DOPC:DOPS adsorption, where significant adsorption and SLB formation only occurs in the presence of Ca^{2+}. Especially for the DOPC:DOPS lipid bilayer both the mass surface density and the orthogonal alignment as interpreted from the changes in n and birefringence increased significantly compared to pure DOPC. The interactions of POPC and POPS with calcium were studied over the last decades. The presence of Ca^{2+} induces structural changes of the hydrocarbon chain packing and of the polar headgroup packing, e.g. inducing changes of the hydration shell. Calcium ions bind naturally to negatively charged phospholipids such as PS. It is well documented that PS molecules are able to form strong molecular complexes with Ca^{2+} ions, leading to complete dehydration of the serine headgroup. It has also previously been shown that Ca^{2+} can mediate a strong interaction of PS lipids with an underlying substrate.[20,21,26] PS lipids will be preferentially organized in the substrate proximal leaflet and can even remain immobile on, e.g., TiO_2 surfaces, which bind Ca^{2+} strongly. Such strong interactions would be expected to influence also the average alignment of lipids, which depending on the angle of the binding of the ion and its interaction with the substrate could lead to an induced average tilt. Our data again indicate a strong influence of Ca^{2+} depending on fatty acid chains of lipids. The two unsaturated alkyl chains of DOPC:DOPS together with Ca^{2+} give rise to a much higher packing (mass density) and orthogonal alignment than for pure DOPC despite their more conical shape factor. While POPC:POPS still shows a high orthogonal alignment, its mass density is decreased compared to pure POPC.

Thermal Effects on SLB. Changing an SLB from the lamellar liquid crystalline phase to the gel phase will change not only the fluidity of the membrane but also the packing and thus the alignment of the lipids. This has previously been demonstrated for DMPC supported lipid bilayers deposited by the Langmuir−Blodgett technique.[28] The DMPC bilayer has a phase transition at ~24 °C.[28,53,54]

In order to compare these results with those obtainable with DPI for a self-assembled DMPC supported lipid bilayer, we reduced the temperature for an SLB assembled at 30 to 20 °C. In Table 1 are listed the isotropic refractive index, birefringence and apparent isotropically weighted thickness, calculated as described for the other lipid systems, for a DMPC SLB at the two extreme temperatures (in the absence of Ca^{2+}). As a comparison we also give the thickness and refractive index obtained for adsorption of a full layer of DMPC liposomes at 20 °C, a temperature at which the gel phase liposomes will not rupture to form an SLB. As previously observed by Horváth et al. the SLB at 20 °C is denser and thicker than the SLB in the liquid crystalline state at 30 °C. However, our results differ for the birefringence, where Horváth et al.[28] determine a negative birefringence which decreases further with increased temper-

(49) den Engelsen, D. *Surf. Sci.* **1976**, *56*, 272–280.
(50) Gaines, G. L.; Tabor, D. *Nature* **1956**, *178*, 1304–1305.
(51) Satsangi, A.; Satsangi, N.; Glover, R.; Satsangi, R. K.; Ong, J. L. *Biomaterials* **2003**, *24*, 4585–4589.
(52) Nygren, H.; Tengvall, P.; Lundstrom, I. *J. Biomed. Mater. Res.* **1997**, *34*, 487–492.
(53) Mabrey, S.; Sturtevant, J. M. *Proc. Natl. Acad. Sci. U.S.A.* **1976**, *73*, 3862–3866.
(54) Schuy, S.; Janshoff, A. *ChemPhysChem* **2006**, *7*, 1207–1210.

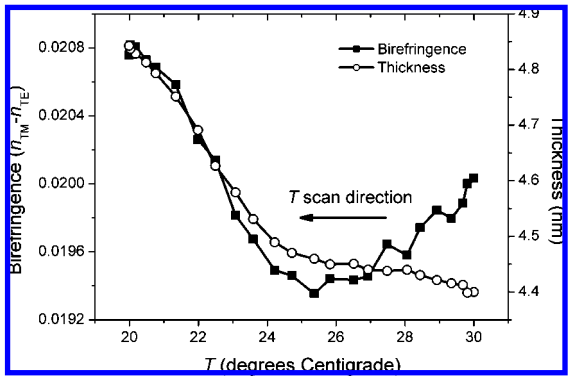

Figure 5. A DMPC supported lipid bilayer formed in the liquid crystalline state by liposome fusion at 30 °C is subjected to a reduction in temperature to 20 °C. A phase transition is observed commencing at $T \approx 24$ °C evidenced by a dramatic increase in lipid bilayer thickness and birefringence. Birefringence and thickness are calculated assuming a constant $n = 1.47378$ obtained for the SLB at 30 °C with temperature lag and effects on the waveguide and bulk solution subtracted by use of the instrument reference channel.

ature. In our measurement the birefringence stays positive at both temperatures and is highest at 20 °C. Thus, the trend of change but not the sign and the magnitude agrees with the results reported by Horváth et al. However, we would like to emphasize that although we do not know the cause of this absolute difference in obtained birefringence, the observation of negative optical birefringence by Horváth et al. for the DMPC SLB is an exception in the literature. In other studies of SLBs the results—like for our other lipid systems—have been a positive birefringence.[32,55]

Figure 5 shows the result of reducing the temperature from 30 to 20 °C for the DMPC SLB. To generate this graph the temperature effect on the waveguide structure and the bulk liquid has been accounted for by use of a control measurement in a parallel uncoated reference channel on the waveguide chip. The refractive index change of water is essentially linear with temperature over this temperature range, so the bulk buffer refractive index change has been used to calculate the actual temperature at the surface of the chip, accounting for the effect of thermal hysteresis between the surface of the chip and the thermocouple in the thermal block below the chip. However, we cannot determine simultaneous transient changes in SLB thickness and refractive index/birefringence without measuring an additional parameter, so in order to obtain the birefringence the refractive index, n, is kept constant for the modeling at the value determined for the 4.4 nm SLB at 30 °C ($n = 1.47378$). This is presumably the reason for the apparent decrease in birefringence as the temperature drops from 30 to 25 °C, where the density would be increasing, before the phase transition as well as after the phase transition, where density and thicknesses rises dramatically. This will also result in an underestimation of the birefringence below the phase transition where the density of the membrane increases. The phase transition is easily observed at $T \approx 24$ °C also from the birefringence data. The onset of the phase transition is sharply defined at just above 24 °C, but the transition is drawn out in the temperature scanning direction toward 20 °C. This may be evidence of the presence of the premelt ripple gel phase.[56,57] Nonetheless, the low temperature and relatively sharp transition reflect a mobile bilayer relatively unconstrained by interactions with the underlying surface.[54]

CONCLUSIONS

Allowing for anisotropic layers enables determination of birefringence of bilayer together with thickness or refractive index (with the other a fixed value). This approach removes differences in mass loading due to anisotropy, so the mass becomes solely a function of the lipid dn/dc value or molar refractivity.

We have also demonstrated that DPI—and therefore other waveguide spectroscopy configurations with comparable sensitivity—with rate of mass adsorption and birefringence analysis can be used to sensitively detect the different stages of SLB formation from liposomes, which have previously not been demonstrated for a label free optical evanescent technique. The method is general and can be applied to any system undergoing structural transformations during adsorption between states with differences in terms of polarizability of the film for the two waveguide modes. A detailed analysis by this approach revealed new findings such as different adsorption kinetics for zwitterionic PC liposomes and net negatively charged PS-containing liposomes at the same bulk concentration and a higher propensity for fluctuations in cluster rupture size for PC vesicles in the absence of Ca^{2+} than for systems without Ca^{2+}. These findings strongly indicate that correlation of adsorption sites due to mutual liposome charge repulsion is important to understand the detailed adsorption and SLB formation kinetics. The results also indicate that even for SLB forming systems that due to charge differ significantly in surface interaction the critical liposome coverage is very similar. We could also demonstrate that the high sensitivity to average lipid tilt angle could be used to measure a strong influence of especially the number of unsaturated alkyl chains on the density and order of the formed SLB in the presence of Ca^{2+}, and furthermore show that the assembly method can have a large influence on the lipid density and order by comparing our results to previously published results for POPC membranes assembled by other methods. The birefringence and refractive index values presented in Table 1 are the first presented for solvent-free SLBs self-assembled through the increasingly popular liposome fusion method. The applicability of our analysis to measure the drastic change of optical and structural properties of an SLB when it goes through the gel-liquid phase transition was also demonstrated.

The application of waveguide spectroscopy to study conformational changes and detailed molecular alignment in real time, as applied here by DPI to SLB formation kinetics and characterization of SLB properties, also has great potential to study transitions in supported membranes caused by biologically

(55) Ramsden, J. J. *Philos. Mag. B—Phys. Condens. Matter Stat. Mech. Electron. Opt. Magn. Prop.* **1999**, *79*, 381–386.

(56) Enders, O.; Ngezahayo, A.; Wiechmann, M.; Leisten, F.; Kolb, H. A. *Biophys. J.* **2004**, *87*, 2522–2531.

(57) Kaasgaard, T.; Leidy, C.; Crowe, J. H.; Mouritsen, O. G.; Jorgensen, K. *Biophys. J.* **2003**, *85*, 350–360.

relevant processes like membrane-interacting peptides or membrane active drugs. It could also easily be applied to other systems for which order transitions occur affecting the optical properties.

ACKNOWLEDGMENT

The authors from ETH Zurich acknowledge Swiss Competence Center for Materials Research (CCMX) and EU FP7 Grant ASMENA for funding. The authors from Farfield Group Ltd acknowledge UK BBSRC SBRI scheme for financial support and Dr. G. H. Cross (University of Durham) for help with the waveguide theory.

Received for review January 6, 2008. Accepted March 17, 2008.

AC800027S